Commun. Theor. Phys. **68** (2017) 259–268 Vol. 68, No. 2, August 1, 2017

Physical Properties of C-Si Alloys in $C2/m$ Structure*

Qian-Kun Wang (王乾坤), Chang-Chun Chai (柴常春), Qing-Yang Fan (樊庆扬),† and Yin-Tang Yang (杨银堂)

Key Laboratory of Ministry of Education for Wide Band-Gap Semiconductor Materials and Devices, School of Microelectronics, Xidian University, Xi'an 710071, China

(Received March 7, 2017; revised manuscript received May 4, 2017)

Abstract *Using the first principles calculations based on density functional theory, the crystal structure, elastic anisotropy, and electronic properties of carbon, silicon and their alloys ($C_{12}Si_4$, C_8Si_8, and C_4Si_{12}) in a monoclinic structure ($C2/m$) are investigated. The calculated results such as lattice parameters, elastic constants, bulk modulus, and shear modulus of C_{16} and Si_{16} in $C2/m$ structure are in good accord with previous work. The elastic constants show that C_{16}, Si_{16}, and their alloys in $C2/m$ structure are mechanically stable. The calculated results of universal anisotropy index, compression and shear anisotropy percent factors indicate that C-Si alloys present elastic anisotropy, and C_8Si_8 shows a greater anisotropy. The Poisson's ratio and the B/G value show that C_8Si_8 is ductile material and other four C-Si alloys are brittle materials. In addition, Debye temperature and average sound velocity are predicted utilizing elastic modulus and density of C-Si alloys. The band structure and the partial density of states imply that C_{16} and Si_{16} are indirect band gap semiconductors, while $C_{12}Si_4$, C_8Si_8, and C_4Si_{12} are semi-metallic alloys.*

PACS numbers: 71.22.+i, 61.50.-f, 71.55.Cn **DOI:** 10.1088/0253-6102/68/2/259
Key words: C-Si alloys, elastic properties, anisotropic properties, electronic properties

1 Introduction

Group-IV semiconductors (C, Si, and Ge) have been the subject of a considered amount of experimental and theoretical studies due to their special physical properties and chemical properties.[1−11] Their alloys, C-Si and Si-Ge, have also been attracted increasingly interest and been searched over the past decades.[12−20] Tang *et al.*[5] found that nt-p-Si structure (belongs to $I4_1$/amd space group) possesses a direct band gap wider by 0.5 eV than the indirect one of silicon with diamond structure and shows anisotropic optical properties and Young modulus. The bulk modulus (64.4 GPa) and the density (1.9 g/cm3) are also lower than that of diamond silicon. The mechanical and electronic properties of Si-Ge alloys in $Cmmm$ structure, $P2221$ structure, and $P4_2/mnm$ structure were calculated and discussed in Refs. [12–14], respectively. Damien *et al.*[15] reported a study of carbon and silicon chiral framework structures (CFSs) properties, as their band structure calculations show, the band gaps of C- and Si-CFSs are 5.5 eV and 1.8 eV, respectively. In their research, silicon presents an unusually low frequency of higher modes at Γ point. Li *et al.*[16] discussed a novel phase carbon possessing a monoclinic of $C2/m$ structure (8 atoms per cell) identified utilizing an *ab initio* evolutionary structural search, which indicated that it is stable over cold-compressed graphite above 13.4 GPa, and hardness and bulk modulus are 83.1 GPa and 431.2 GPa, respectively. Tan *et al.*[17] studied the crystal structural, elastic anisotropy and electronic properties of C-Si alloys in the $P222_1$ structure, the results show that Si_{10} is an indirect semiconductor with a band gap of 0.93 eV and C-Si alloys are elastic anisotropies. Zhang *et al.*[18] investigated the structural, elastic, and electronic properties of two new Si_8C_4 and Si_4C_8 (belong to $P4_2//mnm$ space) using the first principles calculations. They found that Si_8C_4 and Si_4C_8 are mechanically and dynamically stable, and present an elastic anisotropy. In addition, Si_8C_4 and Si_4C_8 are indirect semiconductors with values of 0.74 eV and 0.15 eV, respectively. Xing *et al.*[19] have explored, by the first-principles calculations, the mechanical properties and electronic properties of $C2/m$ carbon, the elastic constants reveal that $C2/m$ carbon is mechanically stable according to the elastic stability criteria under pressure, and their calculations also show that $C2/m$ carbon has a band gap of 4.197 eV. Fan *et al.*[20] optimized and calculated the structure, elastic constants, Debye temperature and electronic properties of $C2/m$ silicon, the calculated results manifest that $C2/m$ silicon is mechanically stable and also thermodynamic stable. $C2/m$ silicon is an indirect semiconductor with a narrow band gap of 0.561 eV, and the Debye temperature is 574 K.

The crystal structure, elastic anisotropy properties and electronic properties of C_{16} and Si_{16} in $C2/m$ structure were predicted in Refs. [19] and [20], respectively, but these properties of $C_{12}Si_4$, C_8Si_8, and C_4Si_{12} have not been studied. In this work, the crystal structures of C_{16},

*Supported by the Natural Science Foundation of China under Grant No. 61474089, Open Fund of Key Laboratory of Complex Electromagnetic Environment Science and Technology, China Academy of Engineering Physics under Grant No. 2015-0214. YY.K

†Corresponding author, E-mail: qyfan_xidian@163.com

Si_{16} and their alloys ($C_{12}Si_4$, C_8Si_8, and C_4Si_{12}) in $C2/m$ phase are built up and optimized utilizing first principle calculations, the elastic anisotropy indexes, Vickers hardness, average sound velocity, and Debye temperature are obtained and analyzed. Furthermore, the band gaps and partial density of states of C-Si alloys are also investigated.

2 Computational Details and Theory

In this paper, all calculations are performed by using the density functional theory (DFT),[21−22] integrated in the Cambridge Serial Total Energy Package (CASTEP) code.[23] The exchange and correlation are approximated by the generalized gradient approximation (GGA) in the form of Perdew, Burke and Ernzerrof (PBE),[24] PBEsol,[25] and local density approximation (LDA) in the form of Ceperley and Alder data as parameterized by Perdew and Zunger (CA-PZ).[26−27] The Broyden–Fletcher–Goldfarb–Shanno (BFGS)[28] minimization scheme was used in geometry optimization. The interactions between the ionic core and valence electrons were described by the Ultra-soft pseudo-potential. The valence electron configurations of C and Si atoms are $2s^2 2p^2$ and $3s^2 3p^2$, respectively. For C_{16}, Si_{16}, and their alloys in $C2/m$ structure, a plane-wave basis set with energy cut-off 400 eV, 340 eV, and 400 eV are used, respectively. The k-points in the first Brillouin zone[29] were $14 \times 7 \times 9$, $12 \times 6 \times 8$, $12 \times 7 \times 8$, $13 \times 7 \times 9$, and $13 \times 7 \times 9$ for C_{16}, Si_{16}, $C_{12}Si_4$, C_8Si_8, and C_4Si_{12}, respectively. The self-consistent convergence of the total energy is 5×10^6 eV/atom, the maximum force on the atom is 0.01 eV/Å, the maximum stress within 0.02 GPa and the maximum ionic displacement within 5×10^{-4} Å.

3 Results and Discussion

The crystal structures of C_{16}, Si_{16}, and their alloys ($C_{12}Si_4$, C_8Si_8, and C_4Si_{12}) are shown in Fig. 1. These crystal structures belong to monoclinic symmetry, with the space of $C2/m$. There are 16 atoms in a conventional cell and connect to each other through C-C, C-Si, or Si-Si bonds. After optimization, the calculated lattice parameters for C-Si alloys are listed in Table 1, and the calculated results are in accord with the available referenced data.[14,19−20,30−35] As Table 1 and Fig. 2 show, the values of lattice parameters (a, b, and c) and volumes have a growing trend with the Si composition increasing. Besides, from Table 1, for Si-I (space group: Fd-3m), the lattice parameter calculated by PBE method is in agreement with experimental value compared with PBEsol method and CA-PZ method, so we will use the obtained results from the PBE method in the following discussion because lattice parameters are underestimated in CA-PZ method compared with PBE method.

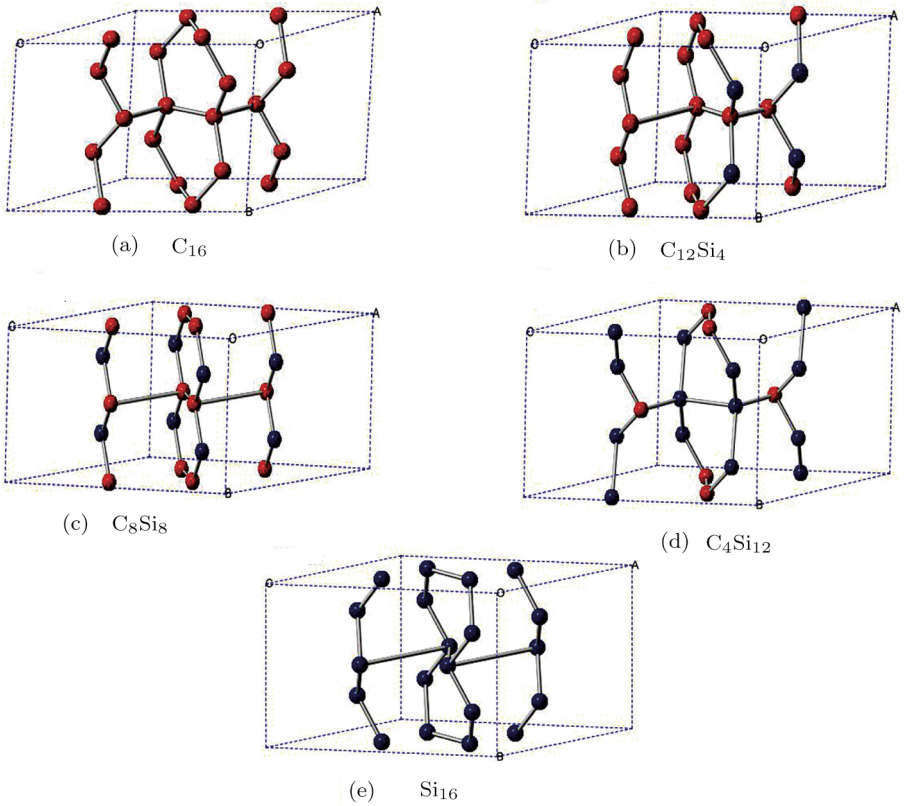

Fig. 1 (Color online) Perspective view of the $C2/m$ C-Si alloys. The red and blue balls represent C atoms and Si atoms, respectively.

Table 1 The calculated lattice parameters (in Å) and β (in °) of C_{16}, $C_{12}Si_4$, C_8Si_8, C_4Si_{12}, and Si_{16} in $C2/m$ structure.

	PBE				PBEsol				CA-PZ			
$C2/m$	a	b	c	β	a	b	c	β	a	b	c	β
C_{16}	4.718	5.045	7.147	146.1	4.704	5.030	7.131	146.1	4.662	6.986	7.068	146.1
	4.721[a]	5.046[a]	7.154[a]	146.1[a]					4.664[b]	4.986[b]	7.070[b]	146.1[b]
	4.726[c]	5.053	7.161	146.1								
$C_{12}Si_4$	5.895	5.354	8.598	148.9	5.873	5.333	8.571	148.7	5.774	5.292	8.441	148.6
C_8Si_8	7.727	6.303	10.796	153.4	7.680	6.296	10.748	153.3	7.542	6.207	10.568	153.1
C_4Si_{12}	6.686	6.904	10.233	149.5	6.684	6.876	10.236	149.6	6.590	6.777	10.088	149.5
Si_{16}	7.190	7.687	10.928	146.1	7.182	7.660	10.921	146.1	7.075	7.543	10.761	146.1
	7.192[d]	7.677[d]	10.930[d]	146.1[d]								
Fd-3m-Si	$a = 5.460, 5.465$[e], 5.402[f], 5.429[g], 5.465[h]				5.466[e]				$a = 5.374$[e], 5.392[f]			
Exp.	5.430[i]											

[a]Ref. [35]; [b]Ref [19]; [c]Ref. [34]; [d]Ref. [20]; [e]Ref. [14]; [f]Ref. [30]; [g]Ref. [31]; [h]Ref. [32]; [i]Exp[33].

In order to get more information about stability and stiffness of crystals, the calculated elastic constants and the elastic modulus of C-Si alloys in $C2/m$ structure, together with previous data,[20,35] which are shown in Table 2. There are thirteen independent elastic constants in a stable monoclinic structure, and these independent elastic constants should obey the following generalized Born′s mechanical stability criteria:[28]

$$C_{ii} > 0\,, \quad i = 1 \sim 6\,, \tag{1}$$

$$[C_{11} + C_{22} + C_{33} + 2(C_{12} + C_{13} + C_{23})] > 0\,, \tag{2}$$

$$(C_{33}C_{55} - C_{35}^2) > 0\,, \tag{3}$$

$$(C_{44}C_{66} - C_{46}^2) > 0\,, \tag{4}$$

$$(C_{22}C_{33} - C_{23}^2) > 0\,, \tag{5}$$

$$[C_{22}(C_{33}C_{55} - C_{35}^2) + 2C_{23}C_{25}C_{35} - C_{23}^2C_{55} - C_{25}^2C_{33}] > 0\,, \tag{6}$$

$$2[C_{15}C_{25}(C_{33}C_{12} - C_{13}C_{23}) + C_{15}C_{35}(C_{22}C_{13} - C_{12}C_{23}) + C_{25}C_{35}(C_{11}C_{23} - C_{12}C_{13})] - [C_{15}^2(C_{22}C_{33} - C_{23}^2) + C_{25}^2(C_{11}C_{33} - C_{13}^2) + C_{35}^2(C_{11}C_{22} - C_{12}^2)] + C_{55}g > 0\,, \tag{7}$$

$$g = C_{11}C_{22}C_{33} - C_{11}C_{23}^2 - C_{22}C_{13}^2 - C_{33}C_{12}^2 + 2C_{12}C_{13}C_{23} > 0\,, \tag{8}$$

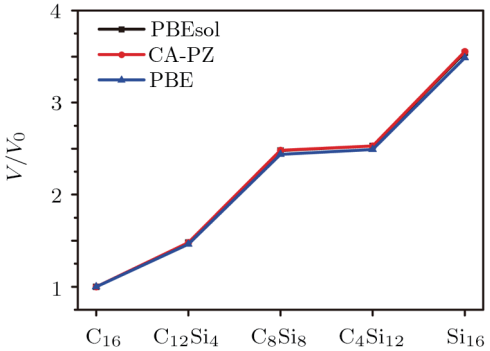

Fig. 2 The volume V/V_0 as functions of the numbers of silicon atoms by PBE, PBEsol and CA-PZ methods.

The independent elastic constants of C_{16}, Si_{16}, and their alloys ($C_{12}Si_4$, C_8Si_8, and C_4Si_{12}) in $C2/m$ structure satisfy the above equations. That is to say, these five crystals in $C2/m$ structure are mechanically stable under ambient condition. To confirm the dynamic stability of C-Si alloys in $C2/m$ phase ($C_{12}Si_4$, C_8Si_8, and C_4Si_{12}), the phonon spectra of $C_{12}Si_4$, C_8Si_8, and C_4Si_{12} are displayed in Fig. 3. There is no imaginary frequency along the whole Brillouin zone from the Fig. 3, which indicate that these alloys are all dynamically stable.

In order to evaluate the relative stability of C-Si alloys, the phase diagram is calculated based on the regular-solution model.[37] The formation energy ΔH of C-Si alloys is defined as follows:

$$\Delta H = E_{\text{total}} - \frac{m}{m+n}E_C - \frac{n}{m+n}E_{\text{Si}}\,, \tag{9}$$

where E_{total} is the total energy of C-Si alloys, m and n are the number C and Si atoms in a conventional cell. The chemical potentials E_{C} and E_{Si} are the total energy of C_{16} and Si_{16}, respectively. The formation energy of C-Si alloys using PBE, PBEsol, and CA-PZ methods are illustrated in Fig. 4. The formation energies are all positive, and the alloys might exist at a specified high temperature scale due to the entropy ΔH effects considered. The Helmholtz free energy ΔG can be expressed as:

$$\Delta G = \Delta E - T\Delta H\,, \tag{10}$$

where ΔE is the internal energy and T is the absolute temperature of the surroundings. In addition, for the regular solution model of alloys, the entropy ΔH can be defined as:

$$\Delta H = -R\Big[\frac{n}{m+n}\ln\Big(\frac{n}{m+n}\Big) + \frac{m}{m+n}\ln\Big(\frac{m}{m+n}\Big)\Big], \tag{11}$$

where R is the gas constant. As Eqs. (10) and (11) show, C-Si alloys in $C2/m$ structure can be synthesized in a high temperature environment.

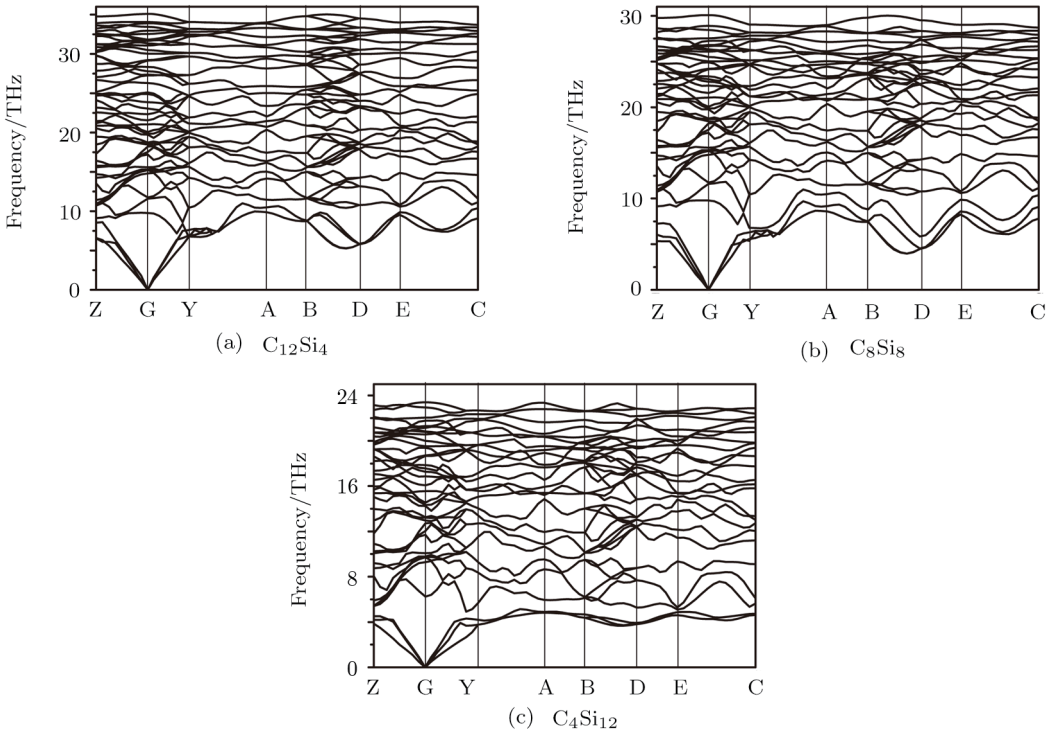

Fig. 3 The phonon spectra of (a) $C_{12}Si_4$, (b) C_8Si_8, and (c) C_4Si_{12}.

Table 2 The elastic constants (in GPa) of C_{16}, $C_{12}Si_4$, C_8Si_8, C_4Si_{12}, and Si_{16} in $C2/m$ structure.

	C_{11}	C_{22}	C_{33}	C_{44}	C_{55}	C_{66}	C_{12}	C_{13}	C_{23}	C_{15}	C_{25}	C_{35}	C_{46}
C_{16}	1021	1028	1017	434	491	458	78	118	73	20	57	2	71
C_{16}[a]	1022	1022	1051	482	482	457	78	116	72	26	54	–1	71
$C_{12}Si_4$	425	544	381	115	154	201	188	128	85	44	37	47	82
C_8Si_8	236	385	128	45	56	111	74	97	30	63	28	7	44
C_4Si_{12}	211	203	248	78	78	80	76	71	42	–5	6	1	10
Si_{16}	152	152	166	49	58	56	47	45	41	1	12	–5	12
Si_{16}[b]	146	146	164	48	53	53	51	47	43				

[a]Ref. [35]; [b]Ref. [20].

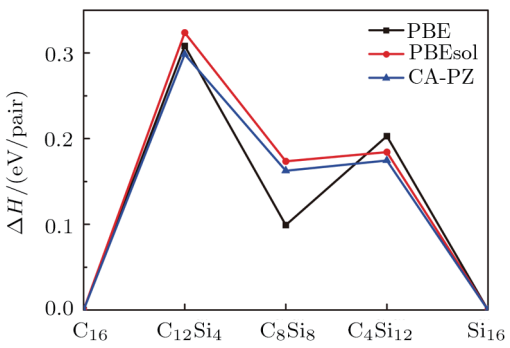

Fig. 4 The formation energy of C-Si alloys.

The elastic constants C_{11}, C_{22}, and C_{33} represent resistance to linear compression along the x, y, and z axis, respectively.[38] As can be seen from Fig. 5(a), the calculated C_{11}, C_{22}, and C_{33} for C_{16} are larger than those of $C_{12}Si_4$, C_8Si_8, C_4Si_{12}, and Si_{16}, which indicates that the x, y, and z axis of C_{16} are more compressible than those of $C_{12}Si_4$, C_8Si_8, C_4Si_{12}, and Si_{16}. In addition, with the composition of Si increasing, C_{11}, C_{22}, and C_{33} become smaller (except for C_{33} of C_8Si_8).

Bulk modulus B and shear modulus G represent resistance to fracture and plastic deformation, respectively. The Voigt–Reuss–Hill approximation[39–41] is adopted to calculate bulk modulus and shear modulus. As Fig. 5(b) shows, there is a trend that bulk modulus and shear modulus decrease with the composition of Si increasing, however, the values of B and G of C_8Si_8 are slightly smaller than those of C_4Si_{12}.

H_V is the Vickers hardness. To a certain extent, H_V can reflect elastic and plastic properties and can be calculated by the following formula:[42]

$$H_{\text{Chen}} = 2(k^2G)^{0.585} - 3\,, \tag{12}$$

in which k is G/B. From Table 3, it can be found that the Vickers hardness of C_{16} (82.1 GPa) is the largest compared with $C_{12}Si_4$ (17.8 GPa), C_8Si_8 (7.5 GPa), C_4Si_{12} (13.2 GPa), and Si_{16} (9.7 GPa). The calculated average C-C bond length for C_{16} is 1.555 Åand average Si-Si bond length for Si_{16} is 2.372 Å, while average C-Si bonds length for $C_{12}Si_4$, C_8Si_8, and C_4Si_{12} are 1.889 Å, 1.888 Å, and 1.965 Å, respectively. As we know, a greater energy is necessary when a shorter chemical bond is disrupted, in other words, C_{16} is the hardest crystal in these five crystals due to C-C bond is the shortest one. Another method proposed by Lyakhov *et al.*[43] is also used to measure the hardness of a solid. The calculated results are shown in Table 3. As we can see that the values of H_{Oganov} become smaller with the silicon increasing, the fact that C-C bond becomes less with silicon increasing may be explain this phenomenon. Besides, obviously, there is a deviation between the results calculated by these two methods for the same material. This is because the value may be too high or too low when an empirical formula is used to calculate the Vickers hardness. Anyhow, C_{16} is super-hard material, while other four materials are not. The Young's modulus E is used to provide a measure of the stiffness of a solid. The larger the value of E is, the stiffer the material is.[44] The Young's modulus E can be calculated by the following equation:[41]

$$E = \frac{9BG}{3B+G}\,. \tag{13}$$

As shown in Fig. 5(b), with the composition of Si increasing, the value of Young's modulus E decrease from 998 GPa to 133 GPa, in addition, the trend of E is accord with that of the bulk modulus B and the shear modulus G.

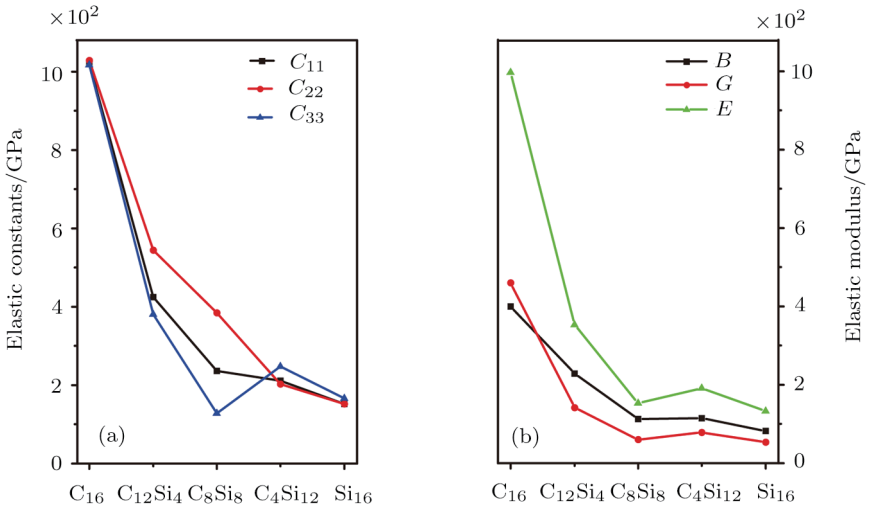

Fig. 5 The elastic constants C_{ij} (in GPa) and elastic modulus (B, G, and E in GPa) of C_{16}, Si_{16}, and C-Si alloys in $C2/m$ structure.

Table 3 The bulk modulus B (GPa), shear modulus G (GPa), B/G, Young's modulus E (GPa), Vickers hardness H_V (GPa) and Poisson's ratio v (m/s) of the $C2/m$ C_{16}, Si_{16} and C-Si alloys.

	B	G	B/G	E	v	H_{Chen}	H_{Oganov}
C_{16}	400	460	0.87	997	0.08	82.1	59.1
	398[a]	458[a]	0.87[a]	993[a]	0.09[a]	89.1[b]	59.5[b]
$C_{12}Si_4$	229	142	1.61	353	0.24	17.8	28.1
C_8Si_8	113	60	1.88	153	0.28	7.5	21.0
C_4Si_{12}	115	78	1.47	191	0.22	13.2	16.0
Si_{16}	82	54	1.52	133	0.23	9.7	9.4
	82[c]	51[c]	1.60[c]	127[c]	0.24[c]		

[a]Ref. [35]; [b]Ref. [34]; [c]Ref. [20].

The ratio of bulk modulus to shear modulus (B/G) is an indicator that can judge a solid is brittle or not according to Pugh's theory,[45] a ductile material has a large B/G value ($B/G > 1.75$), while a brittle material has a small B/G value ($B/G < 1.75$). Poisson's ratio v is consistent with B/G, which means the ductile compounds with a large v (> 0.26) and the brittle compounds with a small v (< 0.26).[46] Poisson's ratio v can be obtained from the following formula:[41]

$$v = \frac{3B - 2G}{2(3B + G)}\,. \tag{14}$$

From Table 3, it can be found that C_8Si_8 have the largest values of B/G (1.88) and v (0.274), which means C_8Si_8 belongs to ductile material. While other four crystals are brittle materials, and C_{16} has the most brittleness with the smallest values of B/G (0.87) and v (0.084).

The elastic anisotropy of a crystal is a significant character for its closely associated with the reasons of micro-crack in the materials.[47] Compression and shear anisotropy percent factor (A_B and A_G) and universal anisotropy index A^U are used to describe the anisotropy extent, which can be expressed as follows:

$$A_B = \frac{B_V - B_R}{B_V + B_R}\,, \tag{15}$$

$$A_G = \frac{G_V - G_R}{G_V + G_R}\,, \tag{16}$$

$$A^U = 5\frac{G_V}{G_R} + \frac{B_V}{B_R} - 6\,, \tag{17}$$

where B_V (G_V) and B_R (G_R) are bulk modulus (shear modulus) in the Voigt and Reuss approximation,[40] respectively. $A_B = A_G = 0$ means a crystal is elastic isotropy, while $A_B = A_G = 1$ represents a crystal shows the maximum elastic anisotropy.[48] A^U is a better indicator than A_B and A_G, the larger the value of A^U is, the stronger the anisotropy of crystal shows.[49] The calculated A_B, A_G, and A^U are listed in Table 4, and are also depicted in Fig. 6(a). As Fig. 6(a) shows, the elastic anisotropy sequence of these five crystals forms the following order: $C_8Si_8 > C_{12}Si_4 > Si_{16} > C_4Si_{12} > C_{16}$, in other words, the value of A^U for C_8Si_8 (4.925) is larger than that of other four C-Si alloys, which means that C_8Si_8 shows the greatest anisotropy. C_{16} is a slightly anisotropic material due to its value of A^U is only 0.079. Besides, it can be found that the values of A_B, A_G, and A^U have a similar trend.

Table 4 Compression and shear anisotropy percent factors (A_B and A_G), universal anisotropy index (A^U), shear anisotropy factors (A_1, A_2, and A_3).

	C_{16}	$C_{12}Si_4$	C_8Si_8	C_4Si_{12}	Si_{16}
G_V	463	157	79	79	55
G_R	456	127	41	77	53
B_V	400	239	128	116	82
B_R	399	249	98	115	82
A_B	0.002	0.044	0.132	0.003	0.001
A_G	0.007	0.108	0.318	0.013	0.018
A^U	0.079	1.302	4.958	0.133	0.187
A_1	0.963	0.832	1.07	0.986	0.863
A_2	1.035	0.816	0.493	0.853	0.992
A_3	0.967	1.352	0.941	1.227	1.059

To further verify the elastic anisotropy of C-Si alloys along diverse orientations, the shear anisotropy factors are considered in this paper. The shear anisotropy factors (A_1, A_2, and A_3) provide a measure of degree of anisotropy in the bonding between atoms in different planes. For the (100) shear plane between [011] and [010] directions, A_1 is defined by the following equality:[50]

$$A_1 = \frac{4C_{44}}{C_{11} + C_{33} - 2C_{13}} \tag{18}$$

for the (010) shear plane between [101] and [001] directions, A_2 is defined by the following equality:[50]

$$A_2 = \frac{4C_{55}}{C_{22} + C_{33} - 2C_{23}}\,, \tag{19}$$

for the (001) shear plane between [110] and [010] directions, A_3 is defined by the following equality:[50]

$$A_3 = \frac{4C_{66}}{C_{11} + C_{22} - 2C_{12}}\,, \tag{20}$$

the calculated results are listed in Table 4 and depicted in Fig. 6(b). $A_1 = A_2 = A_3 = 1.0$ represents the crystal is isotropic, while the crystal must be anisotropic if any value of A_1, A_2, and A_3 is not equal to 1.0. A smaller deviation from 1.0 represents the crystal performs less as anisotropic material. Figure 6(b) shows that C_{16} has a smaller gap between the anisotropy factors (0.693, 1.035, and 0.967, respectively) to 1.0, which means that C_{16} shows weaker anisotropic at three shear planes. C_8Si_8 shows more ob-

vious elastic anisotropy in the (010) plane than (100) and (001) planes, $C_{12}Si_4$ shows more elastic anisotropy in the (001) plane than (100) and (010) planes, C_4Si_{12} shows more elastic anisotropy in the (001) plane than (010) plane, while Si_{16} shows stronger elastic isotropy in the (100) and (010) planes and weaker anisotropy in the (100) plane.

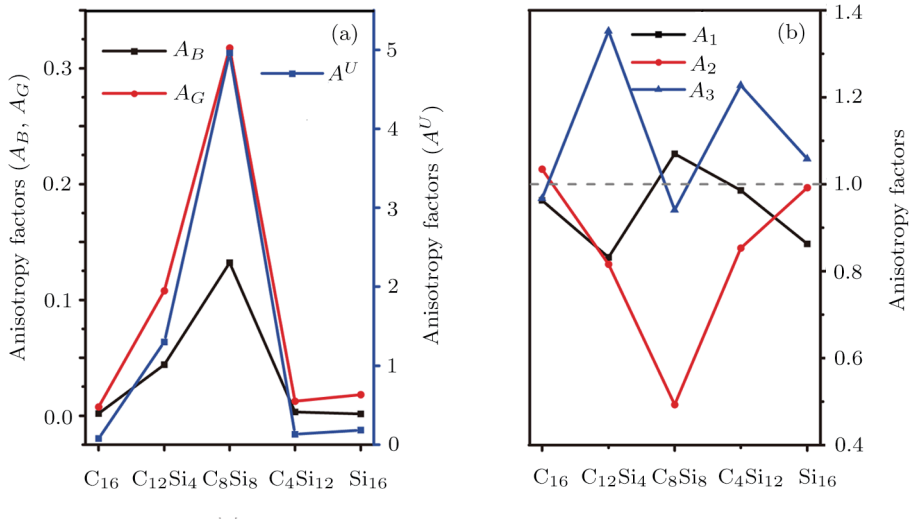

Fig. 6 The universal anisotropic index A^U (in GPa), percent anisotropy A_G and A_B (in GPa) and shear anisotropic factors A_1, A_2, and A_3 of the $C2/m$ C_{16}, Si_{16}, and C-Si alloys.

Table 5 Density (ρ in g/cm^3), shear, compressional and average elastic sound velocities (v_s, v_p, v_m in m/s) as well as Debye temperature (Θ_D in K).

	ρ	v_s	v_p	v_m	Θ_D
C_{16}	3.362	11692	17353	12764	2099
	3.363[a], 3.358[b]	11679[b]	17332[b]	12749[b]	2099[b]
$C_{12}Si_4$	3.305	6839	11741	7587	1095
C_8Si_8	2.264	5145	9234	5729	696
C_4Si_{12}	2.663	5411	9073	5989	723
Si_{16}	2.212	4945	8344	5477	591
	2.217[c]	4796	8225	5320	574

[a]Ref. [35]; [b]Ref. [19]; [c]Ref. [20].

As we know, Debye temperature is an important fundamental parameter closely correlated with many physical properties, such as thermal coefficient, specific heat, dynamic properties, and melting temperature.[51] The Debye temperature Θ_D can be calculated by the following formula:[52]

$$\Theta_D = \frac{h}{k_B}\left[\frac{3n}{4\pi}\left(\frac{N_A\rho}{M}\right)\right]^{1/3} v_m\,, \tag{21}$$

where h is Planck's constant, k_B is Boltzmann's constant, N_A represents Avogadro's constant, n is the number of atoms in the molecule, M is molecular weight, ρ represents the density, and v_m is average sound velocity. v_m can be calculated by the following equation:

$$v_m = \left[\frac{1}{3}\left(\frac{2}{v_t^3} + \frac{1}{v_l^3}\right)\right]^{-1/3}, \tag{22}$$

where v_t and v_l are transverse and longitudinal sound velocities, respectively, which can be calculated by the Navier's equations:[53]

$$v_t = \sqrt{\frac{G}{\rho}}\,, \tag{23}$$

$$v_l = \sqrt{\left(B + \frac{4}{3}G\right)\frac{1}{\rho}}\,, \tag{24}$$

where B and G are bulk modulus and shear modulus, respectively. All of the calculated results are listed in Table 5. It can be found that the order of ρ, v_t, v_m, and Θ_D for C-Si alloys is $C_{16} > C_{12}Si_4 > C_4Si_{12} > C_8Si_8 > Si_{16}$. The order of v_l is $C_{16} > C_{12}Si_4 > C_8Si_8 > C_4Si_{12} > Si_{16}$, which has a small deviation compared with the order of ρ, v_t, v_m, and Θ_D. It is obvious that this trend is the same as the variation trend of the elastic modulus (B, G and E). Theoretically, a stronger interatomic bonding indicates that a crystal has a larger Debye temperature and a higher melting temperature. In fact, the bonds between C atoms are stronger than those of Si atoms, that is to say, Debye temperature of C_{16} must be larger than that of Si_{16} in $C2/m$ structure, obviously, this fact is in accord with the calculated results.

The electric band structure and the partial density of states of the $C2/m$ C-Si alloys calculated by PBE method are presented in Figs. 7 and 8, the dashed lines represent Si_{16} in $C2/m$ structure are 4.20 eV and 0.53 eV, respectively. Besides, the band gaps of C_{16} and Si_{16} are 4.05 eV

(4.15 eV) and 0.44 eV (0.46 eV) calculated by PBEsol method (CA-PZ method), respectively. For C_{16}, the valence band maximum (VBM) is at Z point and the conduction band minimum (CBM) occurs along E-C direction, while the VBM located at Z point and the CBM occurs along B-D direction for Si_{16}, so that C_{16} and Si_{16} are indirect semiconductor. For an indirect band gap semiconductor, there will be phonon emitted during the electronic and momentum is lost, therefore, the luminous efficacy is lower than that of a direct band gap semiconductor, that is to say, C-Si alloys in $C2/m$ structure are not fit for photoelectric devices such as emitting diode. In fact, the true band gaps are larger than the calculated results due to the band gaps calculated by DFT are underestimated. As we can see from Fig. 7, $C_{12}Si_4$, C_8Si_8, and C_4Si_{12} are semimetallic alloys. The bands of $C_{12}Si_4$ are metallic along Z-G and A-D direction with low dispersive bands crossing Fermi level (E_F), while bands of C_4Si_{12} are metallic along Z-Y and D-C direction with higher dispersive bands crossing E_F. It is worth mentioning that only small band gap occurs along Z-G direction showing C_8Si_8 is also metallic as well.

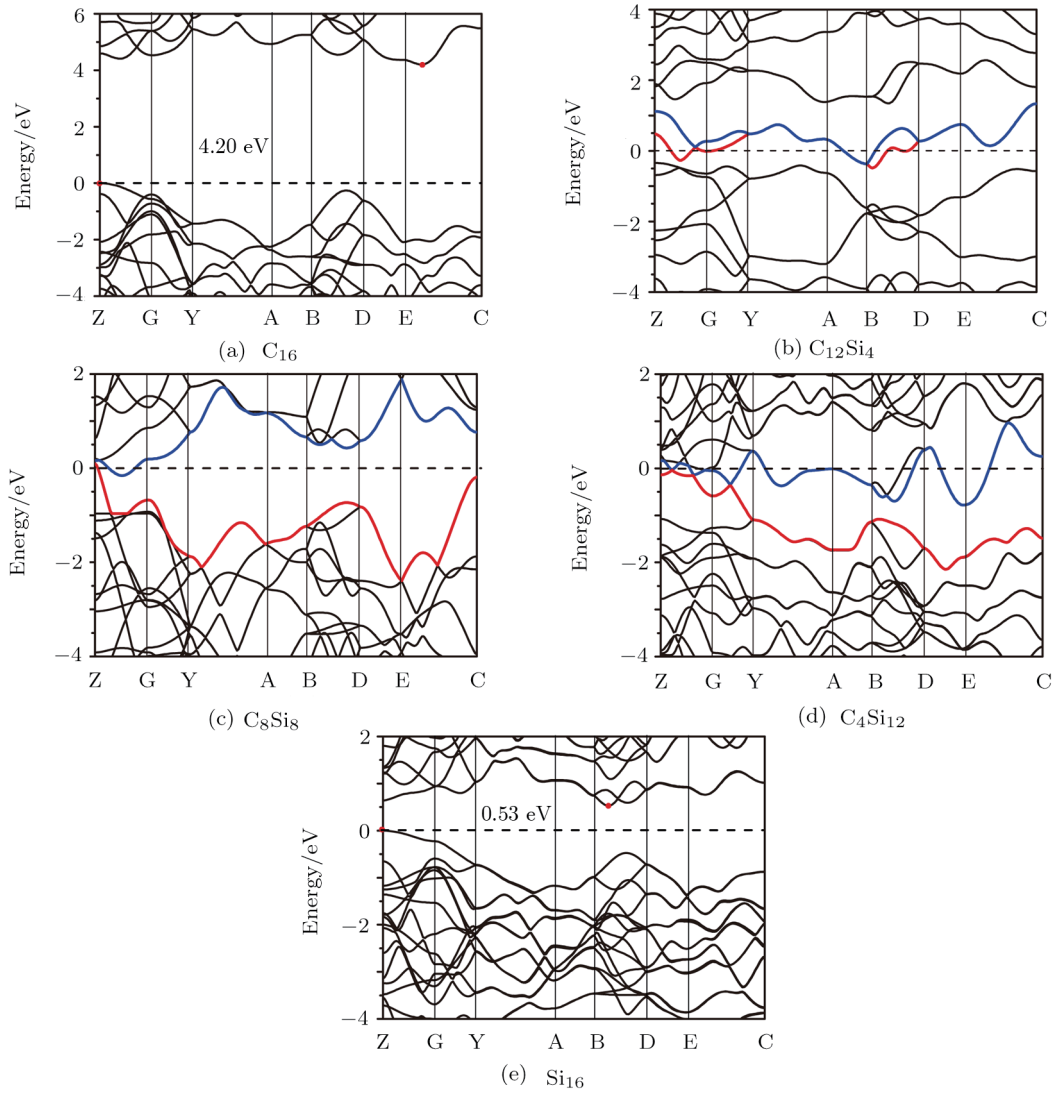

Fig. 7 Electronic band structure of C_{16}, Si_{16} and C-Si alloys in $C2/m$ structure.

The partial density of states (PDOS) per atom in the unit cell for C_{16}, $C_{12}Si_4$, C_8Si_8, C_4Si_{12}, and Si_{16} in $C2/m$ structure are shown in Fig. 8. For $C_{12}Si_4$, $C1$-s, $C2$-s, and $C3$-s represent the s-orbital of carbon atoms located at Wyckoff position $8j$ (in fractional coordinates), $4i$, and $4i$, respectively, and Si1-s represent the s-orbital of silicon atoms located at Wyckoff position $8j$. While $-p$ means the p orbital of atoms. The following features can be seen from Fig. 8, in the range of conduction bands of these five C-Si alloys, the DOS are primary contributed by p states,

mixed with a little s states, while DOSs are mainly featured by s orbital near the bottom of the valence band. For C_8Si_8, the dashed blue line (C2-s) and solid blue line (C2-p) accord exactly with the dashed pink line (C3-s) and solid pink line (C3-p), respectively, which indicates that C2 and C3 play the same role in contributing to the DOSs. In addition, for C_{16} and Si_{16}, the analysis of the top of the valence band show that DOSs are mainly composed of p shell.

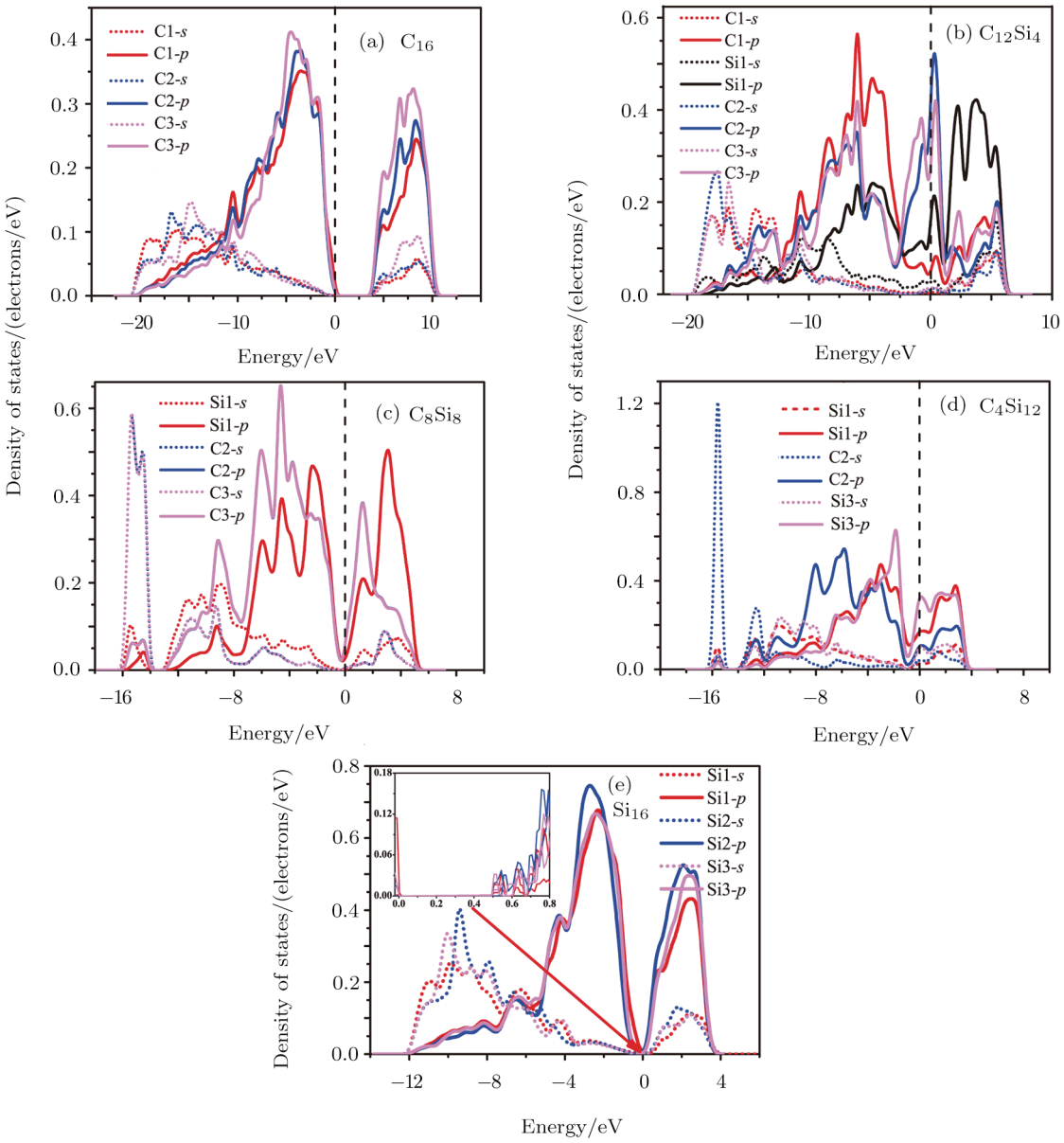

Fig. 8 Density of states of C_{16}, Si_{16} and C-Si alloys in $C2/m$ structure.

4 Summary

In summary, the optimized structural parameters are in agreement with previous work. The elastic constants indicate that $C2/m$ structure is mechanically stable. With the composition of Si increasing, the elastic modulus, shear modulus and Young's modulus present a trend of decreasing (except for C_8Si_8). According to the Vickers hardness, C_{16} is the hardest crystal comparing with other four C-Si alloy. The Poisson's ratio v and the ratio of the bulk modulus to shear modulus indicate that C_8Si_8 belongs to ductile material, while C_{16}, $C_{12}Si_4$, C_4Si_{12}, and Si_{16} belong to brittle material. The compression anisotropy index, shear anisotropy index and universal anisotropy indexes show that C-Si alloys have an elastic anisotropy, the elastic anisotropy sequence forms the following order: $C_8Si_8 > C_{12}Si_4 > Si_{16} > C_4Si_{12} > C_{16}$. The average sound velocities and Debye temperature show a trend of decreasing (except for C_8Si_8)

as the composition of Si increases. Besides, band structures calculations present that $C_{12}Si_4$, C_8Si_8, and C_4Si_{12} are semi-metallic alloys.

References

[1] L. L. Wang and M. Zhao, J. Chem. Phys. **141** (2014) 154505.

[2] M. J. Xing, B. H. Li, Z. T. Yu, and Q. Chen, Commun. Theor. Phys. **64** (2015) 237.

[3] Q. Zhu, O. D. Feya, S. E. Boulfelfel, and A. R. Oganov, J. Super. Mater. **36** (2014) 246.

[4] E. A. Belenkov and V. A. Greshnyakov, Solid State Phys. **57** (2015) 1253.

[5] M. J. Xing, B. H. Li, Z. T. Yu, and Q. Chen, Materials **9** (2016) 484.

[6] A. Mujica, C. J. Picked, and R. J. Needs, Phys. Rev. B **91** (2015) 214104.

[7] M. A. Zwijnenburg, K. E. Jelfs and S. T. Bromley, Phys. Chem. Chem. Phys. **12** (2010) 8505.

[8] M. Amsler, S. Botti, M. A. L. Marques, T. J. Lenosky, and S. Goedecker, Phys. Rev. B **92** (2015) 014101.

[9] M. J. Xing, B. H. Li, Z. T. Yu, and Q. Chen, Eur. Phys. J. B **89** (2016) 9.

[10] A. I. Kochaev, A. A. Karenin, R. M. Meftakhutdinov, and R. A. Brazhe, J. Phys. **345** (2012) 012007.

[11] Q. Zhu, A. R. Oganov, M. A. Salvadó, P. Pertierra, and A. O. Lyakhov, Phys. Rev. B **83** (2011) 193410.

[12] Q. Y. Fan, C. C. Chai, Q. Wei, *et al.*, J. Solid State Chem. **233** (2016) 471.

[13] Y. H. Zhang, C. C. Chai, Q. Y. Fan, and Y. T. Yang, Chinese J. Phys. **54** (2016) 298.

[14] Q. Y. Fan, C. C. Chai, Q. Wei, *et al.*, Mat. Sci. Semicon. Proc. **43** (2016) 187-195.

[15] D. Connétable, Phys. Rev. B **83** (2011) 035206.

[16] Q. Li, Y. M. Ma, A. R. Oganov, *et al.*, Phys. Rev. Lett. **102** (2009) 175506.

[17] L. Tan, C. C. Chai, Q. Y. Fan, and Y. T. Yang, Chinese J. Phys. **54** (2016) 700.

[18] Q. Zhang, Q. Wei, H. Y. Yan, *et al.*, Z. Naturforsch. A **71(5)** (2016) 387.

[19] M. J. Xing, B. H. Li, Z. T. Yu, and Q. Chen, J. Mater. Sci. **50** (2015) 7104.

[20] Q. Y. Fan, C. C. Chai, Q. Wei, *et al.*, J. Appl. Phys. **118** (2015) 185704.

[21] P. Hohenberg and W. Kohn, Phys. Rev. **136** (1964) B864.

[22] W. Kohn and L. J. Sham, Phys. Rev. **140** (1965) A1133.

[23] S. J. Clark, M. D. Segall, C. J. Pickard, *et al.*, Z. Kristallogr. **220** (2005) 567.

[24] J. P. Perdew, K. Burke, and M. Ernzerhof, Phys. Rev. Lett. **77** (1996) 3865.

[25] J. P. Perdew, A. Ruzsinszky, G. I. Csonka, *et al.*, Phys. Rev. Lett. **100** (2008) 136406.

[26] D. M. Ceperley and B. J. Alder, Phys. Rev. Lett. **45** (1980) 566.

[27] J. P. Perdew and A. Zunger, Phys. Rev. B **23** (1981) 5048.

[28] B. G. Pfrommer, M. Côté, S. G. Louie, and M.L. Cohen, J. Comput. Phys. **131** (1997) 233.

[29] J. Moukhorst and J. D. Pack, Phys. Rev. B **54** (1996) 16533.

[30] X. P. Hao, H. L. Cui, and J. Korean, Phys. Soc. **65** (2014) 45.

[31] T. Kumagai, S. Izumi, S. Hara, and S. Sakai, Comput. Mater. Sci. **39** (2007)457.

[32] F. Wu, D. Jun, E. J. Kan, and Z. Y. Li, Solid State Commun. **151** (2011) 1228.

[33] D. R. Lide, Chemical Rubber 73rd ed. Boca Raton, FL: CRC Press (1994).

[34] X. X. Zhang, Y. C. Wang, J. Lv, *et al.*, J. Chem. Phys. **138** (2003) 114101.

[35] M. J. Xing, B. H. Li, Z. T. Yu, and Q. Chen, RSC Adv. **6** (2016) 32740.

[36] Z. J. Wu, E. J. Zhao, H. P. Xiang, *et al.*, Phys. Rev. B **76** (2007) 054115.

[37] R. A. Swalin, *Thermodynamics of Solids*, Wiley, New York (1962).

[38] X. P. Gao, Y. H. Jiang, R. Zhou, and J. Feng, J. Alloys Compd. **587** (2014) 819.

[39] W. Voigt, *Lehrburch der Kristallphysik*, Teubner, Leipzig (1928).

[40] A. Reuss and Z. Angew, Math. Mech. **9** (1929) 49.

[41] R. Hill, Proc. Phys. Soc. London **65** (1952) 349.

[42] X. Q. Chen, H. Niu, D. Li, and Y. Li, Intermetallics **19** (2011) 1275.

[43] A. O. Lyakhov and A. R. Oganov, Phys. Rev. B **84** (2011) 092103.

[44] N. Korozlu, K. Colakoglu, E. Deligoz, and S. Aydin, J. Alloys Compd. **546** (2013) 157.

[45] S. F. Pugh, Philos. Mag. **45** (1954) 823.

[46] J. J. Lewandowski, W. H. Wang, and A. L. Greer, Philos. Mag. Lett. **85** (2005) 77.

[47] P. Ravindran, F. Lars, P. A. Korzhavyi, B. Johansson, J. Wills, and O. Eriksson, J. Appl. Phys. **84** (1998) 4891.

[48] H. B. Ozisik, K. Colakoglu, and E. Deligoz, Comput. Mater. Sci. **51** (2012) 83.

[49] S. I. Ranganathan and M. Ostoja-Starzewski, Phys. Rev. Lett. **101** (2008) 055504.

[50] D. Connétable and O. Thomas, Phys. Rev. B **79** (2009) 094101.

[51] Y. J. Hao, X. R. Chen, H. L. Cui, and Y. L. Bai, Phys. B **382** (2006) 118.

[52] O. L. Anderson, J. Phys. Chem. Solids **24** (1963) 909.

[53] K. B. Panda and K. S. Ravi, Comput. Mater. Sci. **35** (2006) 134.